BULLETIN OF THE POLISH ACADEMY OF SCIENCES
TECHNICAL SCIENCES, Vol. 63, No. 2, 2015
DOI: 10.1515/bpasts-2015-0048

On simplified forms of the fractional-order backward difference and related fractional-order linear discrete-time system description

P. OSTALCZYK*

Institute of Applied Computer Science, Lodz University of Technology, 18/22 Stefanowskiego St., 90-924 Łódź, Poland

Abstract. In this paper three simplified forms of the fractional-order (FO) backward difference (BD) are proposed and analysed. Due to time and frequency characteristics criteria parameters of simplified forms of the FOBDs are chosen. Applications of the simplified forms of the FOBDs diminish a number of multiplications and additions needed to evaluate the FOBD. This is very important in real-time microprocessor calculations. It is proved that in a discrete state-space description of a fractional-order system one should correct the input matrix with simplified forms of the FOBD. Investigations are supported by two numerical examples.

Key words: fractional calculus, discrete-time system response.

1. Introduction

The fractional calculus and fractional differential equations [1–5] as a very potential mathematical tool in different areas of engineering and science is applied to create more adequate models of real dynamical systems. In automatics it may be used to create more sophisticated control strategies. The discretised FO left derivative – the FOBD is a generalisation of commonly known difference or sum. Adequate mathematical models and sophisticated control strategies causes yet simulation problems due to so called "growing calculation tail" threatening to overrun the processor memory. As a remedy for the mentioned disadvantage one can apply a simplified form of the FOBD. This leads to a non-free of calculation errors FOBD approximation. A commonly used approximation consists of a simple cut of an infinite series representing the FOBD. However, this can cause large errors, especially in the case of dynamic systems which are on a stability margin. A paper is organised as follows. In Sec. 2 a definition of the FOBD in Grünwald-Letnikov and Horner forms is given [6]. Some properties of coefficients defining the mentioned forms are given. In Sec. 3 the simplified forms of the FOBD are proposed and discussed its frequency characteristics. Next the simplified forms are used in the FO linear time-invariant systems. An input matrix correction formula is derived. Investigations are supported by numerical examples.

2. Mathematical preliminaries

In this Section, two equivalent forms of the FOBD are introduced. First form is commonly known as the Grünwald-Letniov FOBD [7], the second one as the Horner form [8]. It is worth noting that for the negative FOs, both forms of the FOBD define the fractional-order backward sum (FOBS).

2.1. The Grünwald-Letnikov form of the FOBD.

One defines the FOBD of a discrete-time bounded function f_k as a discrete convolution sum

$$\begin{aligned} {}_0^{GL}\Delta_k^{(\nu)} f_k &= a_k^{(\nu)} * f_k = \sum_{i=0}^{k} a_i^{(\nu)} f_{k-i} \\ &= \begin{bmatrix} a_0^{(\nu)} & a_1^{(\nu)} & \dots & a_{k-1}^{(\nu)} & a_k^{(\nu)} \end{bmatrix} \begin{bmatrix} f_k \\ f_{k-1} \\ \vdots \\ f_1 \\ f_0 \end{bmatrix}, \end{aligned} \tag{1}$$

where the second function is defined below

$$a_k^{(\nu)} = (-1)^k \binom{\nu}{k} = \begin{cases} 1 & \text{for} \quad k = 0 \\ (-1)^k \dfrac{\nu(\nu-1)\dots(\nu-k+1)}{k!} & \text{for} \quad k = 1, 2, 3, \dots \end{cases} \tag{2}$$

$\nu \in R_+$ denotes an order and * denotes a discrete convolution.

2.2. The Horner form of the FOBD.

The Horner form of the FOBD of the discrete-time bounded function f_k is expressed as

$$\begin{aligned} {}_0^{H}\Delta_k^{(\nu)} f_k &= f_k + c_1^{(\nu)} \\ &\cdot \left(f_{k-1} + c_2^{(\nu)} \left(f_{k-2} + c_3^{(\nu)} \left(f_{k-3} + \dots + \left(c_k^{(\nu)} f_0 \right) \right) \right) \right), \end{aligned} \tag{3}$$

where

$$c_k^{(\nu)} = \frac{a_k^{(\nu)}}{a_{k-1}^{(\nu)}} = 1 - \frac{\nu+1}{k}. \tag{4}$$

*e-mail: postalcz@p.lodz.pl

Obviously

$$\lim_{k\to\infty} c_k^{(\nu)} = \lim_{k\to\infty}\left(1-\frac{\nu+1}{k}\right) = 1. \tag{5}$$

From formulae (2) and (4) one obtains

$$\lim_{k\to\infty}\frac{a_k^{(\nu)}}{a_{k-1}^{(\nu)}} = \lim_{k\to\infty} c_k^{(\nu)} = 1 \tag{6}$$

and

$$\lim_{k\to\infty}\frac{c_k^{(\nu)}}{c_{k-1}^{(\nu)}} = \lim_{k\to\infty}\frac{1-\frac{\nu+1}{k}}{1-\frac{\nu+1}{k+1}} = 1. \tag{7}$$

2.3. Coefficients $a_k^{(\nu)}$ and $c_k^{(\nu)}$ selected properties. In computer evaluation of the FOBD the knowledge concerning the convergence of the functions $a_k^{(\nu)}$ and $c_k^{(\nu)}$ is very important. Such information provides inter alia, the first-order difference and the ratio of coefficients $a_k^{(\nu)}$ and $c_k^{(\nu)}$.

Theorem 1. For $0 < \nu < 1$

$${}_0^{GL}\Delta_k^{(1)} a_k^{(\nu)} < {}_0^{GL}\Delta_k^{(1)} c_k^{(\nu)}. \tag{8}$$

Proof. By definition formula (2), for $k = 1, 2, \cdots$

$$\begin{aligned} {}_0^{GL}\Delta_k^{(1)} a_k^{(\nu)} &= a_k^{(\nu)} - a_{k-1}^{(\nu)} \\ &= a_{k-1}^{(\nu)}\left(1-\frac{\nu+1}{k}\right) - a_{k-1}^{(\nu)} \\ &= -\frac{\nu+1}{k} a_{k-1}^{(\nu)} = a_k^{(\nu+1)} > 0. \end{aligned} \tag{9}$$

Similarly, by (4)

$$\begin{aligned} {}_0^{GL}\Delta_k^{(1)} c_k^{(\nu)} &= c_k^{(\nu)} - c_{k-1}^{(\nu)} \\ &= \left(1-\frac{\nu+1}{k}\right) - \left(1-\frac{\nu+1}{k-1}\right) = \frac{\nu+1}{k(k-1)} > 0 \end{aligned} \tag{10}$$

$$\text{for} \quad k = 2, 3, \ldots.$$

Now one examines inequality (8). Substitution (2) into (9) and comparison with (10) yields

$$\begin{aligned} &(-1)\frac{(\nu+1)}{k}(-1)^{k-1}\frac{\nu(\nu-1)\cdots(\nu-k+2)}{(k-1)!} \\ &= (-1)^k\frac{(\nu+1)\nu(\nu-1)\cdots(\nu-k+2)}{k!} < \frac{\nu+1}{k(k-1)}. \end{aligned} \tag{11}$$

The above inequality holds because it may also be expressed in a simplified form

$$(-1)^k\nu\left(\frac{\nu}{1}-1\right)\left(\frac{\nu}{2}-1\right)\cdots\left(\frac{\nu}{k-2}-1\right) < 1 \tag{12}$$

$$\text{for} \quad k = 2, 3, \ldots$$

and further

$$\nu\left(1-\frac{\nu}{1}\right)\left(1-\frac{\nu}{2}\right)\cdots\left(1-\frac{\nu}{k-2}\right) < 1 \tag{13}$$

$$\text{for} \quad k = 2, 3, \ldots.$$

All factors on the left-hand side of inequality (13) are less than 1 which prove the theorem.

The next theorem may be useful in an estimation of the coefficients $a_k^{(\nu)}$ and $c_k^{(\nu)}$ convergence.

Theorem 2. For $0 < \nu < 1$

$$\left|\frac{a_k^{(\nu)}}{a_{k-1}^{(\nu)}}\right| < \left|\frac{c_k^{(\nu)}}{c_{k-1}^{(\nu)}}\right| \quad \text{for} \quad k = 3, 4, \ldots. \tag{14}$$

Proof. By definition formulae (2) and (4)

$$\left|\frac{c_k^{(\nu)}}{c_{k-1}^{(\nu)}}\right| = \left|\frac{1-\frac{\nu+1}{k}}{1-\frac{\nu+1}{k-1}}\right| = \left|1-\frac{\nu+1}{k}\right|\left|\frac{1}{1-\frac{\nu+1}{k-1}}\right|, \tag{15}$$

$$\left|\frac{a_k^{(\nu)}}{a_{k-1}^{(\nu)}}\right| = \left|1-\frac{\nu+1}{k}\right|. \tag{16}$$

Hence,

$$\left|\frac{c_k^{(\nu)}}{c_{k-1}^{(\nu)}}\right| = \left|\frac{a_k^{(\nu)}}{a_{k-1}^{(\nu)}}\right|\left|\frac{1}{1-\frac{\nu+1}{k-1}}\right| \quad \text{for} \quad k = 3, 4, \ldots. \tag{17}$$

Noting that

$$\left|\frac{1}{1-\frac{\nu+1}{k-1}}\right| > 1 \quad \text{for} \quad k = 3, 4, \ldots. \tag{18}$$

one obtains (14).

In view of the Theorems 1 and 2 one can conclude that the convergence of $c_k^{(\nu)}$ to 1 is quicker then $a_k^{(\nu)}$ to 0.

3. Simplified Grünwald-Letniov and Horner forms of the FODS

In microprocessor evaluation of the FOBD due to (1) or (3) it is practically impossible to obtain a precise value. This is caused by a linearly increasing number of multiplications and additions during the FOBD calculation process. In this Section the FODS simplified forms which partially extract mentioned above problems are proposed and discussed. First the most commonly used form is presented

$$a_{1,k}^{(\nu)} = \begin{cases} a_k^{(\nu)} & \text{for} \quad 0 \le k \le L \\ 0 & \text{for} \quad L < k \end{cases}. \tag{19a}$$

In a second proposed simplified form, with two predefined integers L, l one defines coefficients

$$a_{2,k}^{(\nu)} = \begin{cases} a_k^{(\nu)} & \text{for} \quad 0 \le k \le L \\ \widetilde{a}_{j,L}^{(\nu)} & \text{for} \quad jL < k \le t(j+1)L,\ j = 1, 2, \ldots, l \\ 0 & \text{for} \quad (l+1)L < k \end{cases} \tag{19b}$$

for $a_{jL+1}^{(\nu)} \le \widetilde{a}_{j,L}^{(\nu)} \le a_{(j+1)L}^{(\nu)}$, $j = 1, 2, \ldots L-1$. The third simplified form is a special case of (19b)

$$a_{3,k}^{(\nu)} = \begin{cases} a_k^{(\nu)} & \text{for} \quad 0 \le k \le L \\ \widetilde{a}_{l,L}^{(\nu)} & \text{for} \quad L < k \le lL \\ 0 & \text{for} \quad (l+1)L < k \end{cases} \tag{19c}$$

for $a_{L+1}^{(\nu)} \le \widetilde{a}_{l,L}^{(\nu)} \le a_{(l+1)L}^{(\nu)}$.

The idea of approximations consists on cutting a series of coefficients $a_{i,k}^{(\nu)}$ into l parts and partial substitution by constant values. The approximation idea is clarified in Fig. 1 where plots of exact coefficients evaluated according to (2) (in red) and their approximations due (19b) (in blue) and (19c) (in magenta) for $\nu = 0.5$, $L = 50$, $l = 5$ are presented. For a better clarity of coefficients values relations their absolute value logarithms put together are plotted in Fig. 2 for (2) (in red), (19b) (in blue), respectively. One can realise that the approximations becomes better for consecutive intervals tending to l Note that in Fig. 1 zeroed coefficients in (19b) and (19c) cannot be plotted because of a nonexistence of a logarithm of a zero.

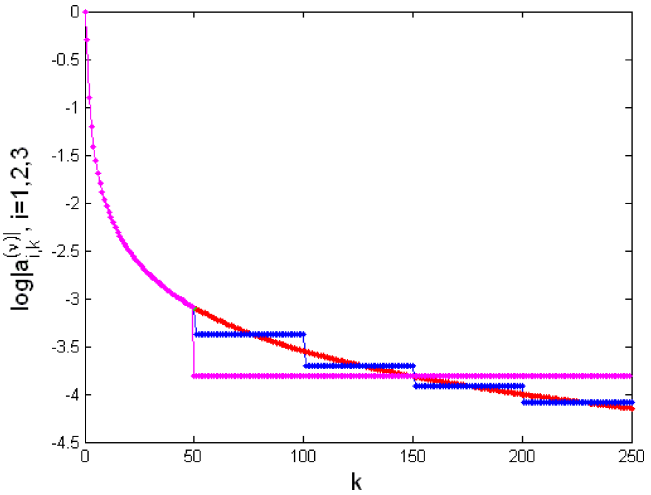

Fig. 1. The logarithms of coefficients (2) (in red), (19b) (in blue) and (19c) (in magenta)

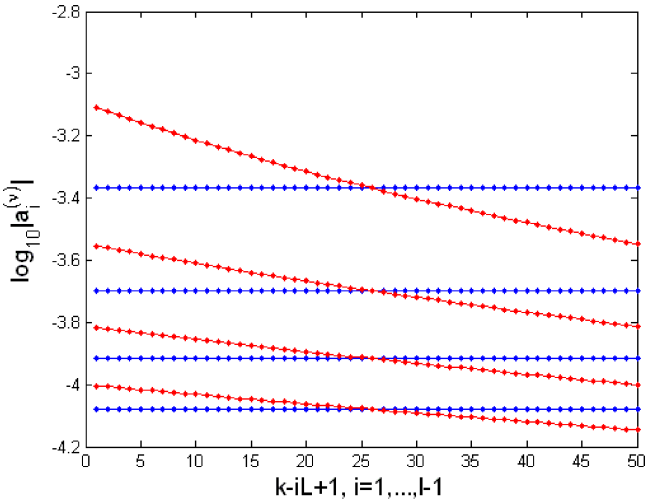

Fig. 2. Logarithms of absolute values of coefficients (2 in red) and their approximation (19b) (in blue)

Simplified coefficients $c_{i,k}^{(\nu)}$ and $\widetilde{c}_{lL,k}^{(\nu)}$ for $i = 1, 2, 3$ and $k = 0, 1, 2, \ldots$ can be evaluated easily from (19a), (19b), (19c) and (2)

Due to the FOBD approximation versions marked by coefficients (19a), (19b), (19c) the simplified forms of the FOBDs are defined:

a) The Grünwald-Letnikov form for $j = 0, 1, 2, 3$

$$ {}_0^{GLj}\Delta_k^{(\nu)} f_k = \sum_{i=0}^{k} a_{j,i}^{(\nu)} f_{k-i}, \tag{20} $$

b) The Horner form for $j = 1, 2, 3$

$$ {}_0^{Hj}\Delta_k^{(\nu)} f_k = f_k + c_{j,1}^{(\nu)} \cdot \left(f_{k-1} + c_{j,2}^{(\nu)} \left(f_{k-2} + c_{j,3}^{(\nu)} \left(f_{k-3} + \cdots + \left(c_{j,k}^{(\nu)} f_0 \right) \right) \right) \right), \tag{21} $$

where $j = 0$ denotes the exact FOBD evaluated accorditn to formulae (1) and (3). In modern microprocessor systems the times of multiplication and addition operations may be assumed to be equal [9]. Hence, one can evaluate the total number of operations required to perform the FOBD calculations according to its simplified forms. The maximal numbers of multiplication and summation operations are collected in Table 1.

Table 1
Multiplication and summation operations for different forms of the FOBD

i	FOBD Form	+	×	Total number of operations $O(i,k)$ for $k > lL$
0	${}_0^{GL}\Delta_k^{(\nu)} f_k$, ${}_0^{H}\Delta_k^{(\nu)} f_k$	k	k	$2k$
1	${}_0^{GL1}\Delta_k^{(\nu)} f_k$, ${}_0^{H1}\Delta_k^{(\nu)} f_k$	$L+1$	$L+1$	$2(L+1)$
2	${}_0^{GL2}\Delta_k^{(\nu)} f_k$, ${}_0^{H2}\Delta_k^{(\nu)} f_k$	$L+l+1$	$Ll+L+1$	$(l+1)L+2(L+1)$
3	${}_0^{GL3}\Delta_k^{(\nu)} f_k$, ${}_0^{H3}\Delta_k^{(\nu)} f_k$	$lL+2$	$L+2$	$(l+1)L+4$

In Fig. 3 multiplications and additions number in the FOBD due to exact (1), (3) (in black) and simplified forms (19b) (red) and (19c) (blue) are plotted.

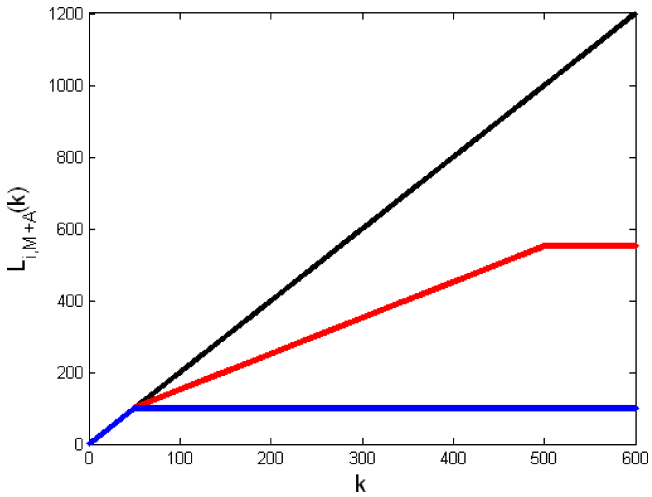

Fig. 3. Multiplications and additions number vs. k for ${}_0^{GL}\Delta_k^{(\nu)} f_k$ (black), ${}_0^{GL1}\Delta_k^{(\nu)} f_k$ (blue) and ${}_0^{GL2}\Delta_k^{(\nu)} f_k$ (red) methods

The simplified forms of the FOBDs (19b) and (19c) in the discrete system description should preserve the system stability conditions [10–13] (asymptotic, marginal stability, instability). There should be a parity between model and their simplified form. The most difficult task is to find a simplified model of the marginally stable system.

4. FOBD simplified forms parameter L and l selection

The one-sided Z-Transform of the FOBD has a form

$$Z\left\{{}_0^{GL}\Delta_k^{(\nu)} f_k\right\} = \Delta(z) = \left(1 - z^{-1}\right)^{\nu} F(z), \tag{22}$$

where $Z\{f_k\} = F(z)$ It can be represented as an infinite series of a complex variable z^{-1}. The simplified forms (19a), (19b), (19c) are represented by finite series

$$Z\left\{{}_0^{GL,j}\Delta_k^{(\nu)} f_k\right\} = \Delta_j(z) = \left[\sum_{i=0}^{lL} a_{j,i}^{(\nu)} z^{-i}\right] F(z) \tag{23}$$

for $j = 1, 2, 3$. Realise that

$$\Delta_4(z) = \left[\sum_{i=0}^{k} a_{j,i}^{(\nu)} z^{-i}\right] F(z) = \lim_{k\to\infty} Z\left\{{}_0^{GL,4}\Delta_k^{(\nu)} f_k\right\}, \tag{24a}$$

$$Z\left\{{}_0^{GL}\Delta_k^{(\nu)} f_k\right\} = \lim_{k\to\infty} Z\left\{{}_0^{GL,4}\Delta_k^{(\nu)} f_k\right\}. \tag{24b}$$

As the FOBD approximation versions (19a), (19b), (19c) criteria may serve the following real functions

$$\begin{aligned} &J_{IAE}\left(L, l, \nu, \widetilde{a}_{lL}^{(\nu)}, i\right) \\ &= \max_{\omega\in[\omega_p,\omega_k]} e_{IAE}\left(L, l, \nu, \widetilde{a}_{lL}^{(\nu)}, \omega, i\right) \\ &= \max_{\omega\in[\omega_p,\omega_k]} \left|\Delta(e^{j\omega}) - \Delta_i\left(e^{j\omega}, L, l\right)\right|, \end{aligned} \tag{25a}$$

$$\begin{aligned} &J_{IsE}\left(L, l, \nu, \widetilde{a}_{lL}^{(\nu)}, i\right) \\ &= \max_{\omega\in[\omega_p,\omega_k]} e_{ISE}\left(L, l, \nu, \widetilde{a}_{lL}^{(\nu)}, \omega, i\right) \\ &= \max_{\omega\in[\omega_p,\omega_k]} \left|\Delta(e^{j\omega}) - \Delta_i(e^{j\omega}, L, l)\right|^2, \end{aligned} \tag{25b}$$

where $\omega_p < \omega_k, \omega_p, \omega_k \in [0\,\pi]$ is a normalised frequency [14] and $i = 1, \ldots, 4$ The shapes of the frequency characteristics of the FOBD (22) and their approximations (23) are presented in a numerical example.

4.1. Numerical example. One considers a fractional order $\nu = 0.5$. In Fig. 4a,b discrete Nyquist diagrams are shown over two frequency ranges $\omega \in [0\,\pi]$ (4a) and $\omega \in [0\,\pi/12]$ (4b): the ideal FOBD described by formula (22) (in black), approximation (19a) for $L = 50$ (in green), approximation (19b) for $L = 50$, $l = 5$ (in blue), (19c) for $L = 50$, $l = 5$, $\widetilde{a}_{lL}^{(\nu)} = a_{150}^{(\nu)}$ (in magenta). Also a plot obtained by formula (1) for $k = 250$ (in red) is added. Figures reveal that approximations acts in a low frequency range.

The plots of the performance criterion $e_{IAE}\left(L, l, \nu, \omega\right)$ (25a) over the second considered range $\omega \in [0\,\pi/12]$ are presented in Fig. 5.

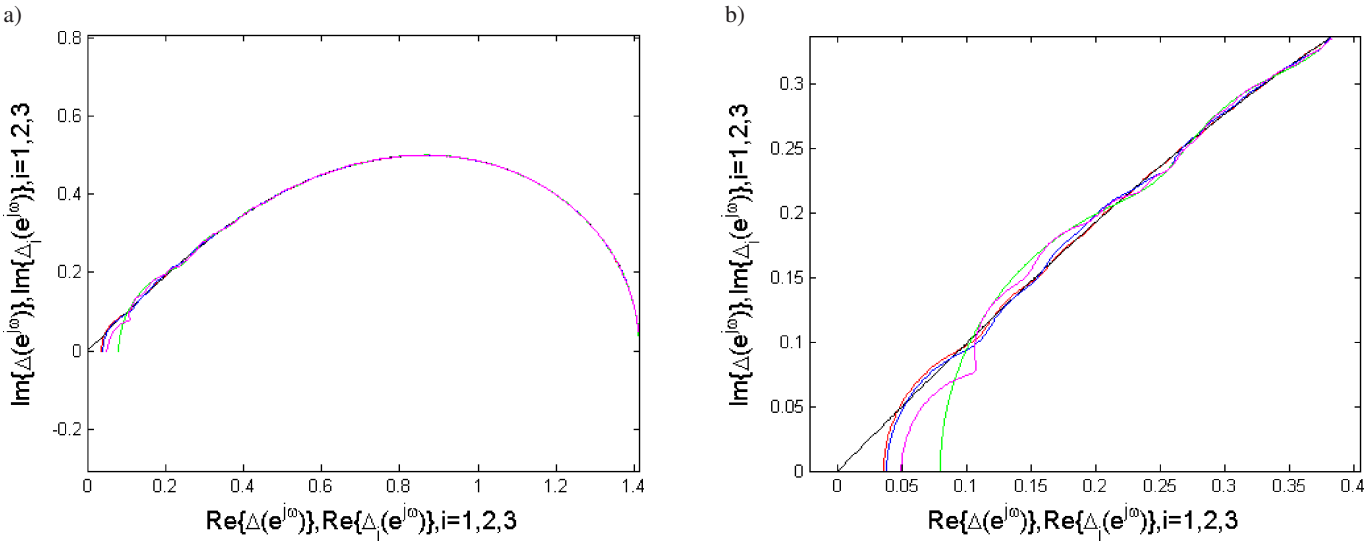

Fig. 4. Discrete Nyquist diagrams of the FOBD (22) – in black and their approximations ((19a) – in green, (19b) – in blue, (19c) – in magenta and (1) – in red) over frequency range $\omega \in [0\,\pi]$ (a) and $\omega \in [0\,\pi/12]$ (b)

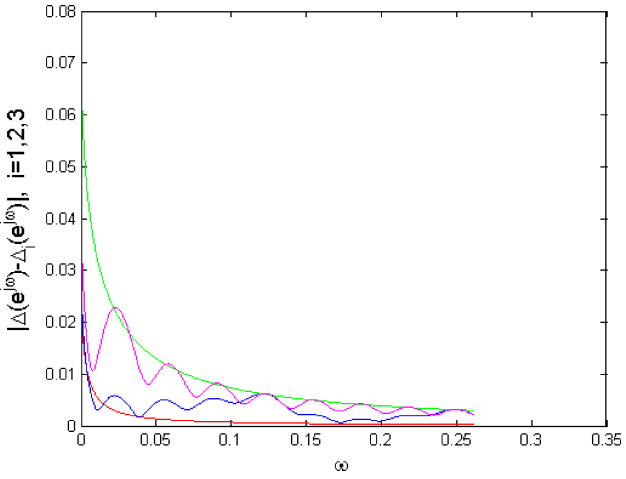

Fig. 5. Performance criterion (25a) vs. frequency of approximations described by formulae ((19a) – in green, (19b) – in blue, (19c) – in magenta and for (1) – in red)) over frequency range $\omega \in [0\,\pi/12]$

5. Linear discrete-time fractional-order system description

The mostly considered description of the linear discrete-time FO system (FOS) is as follows [1, 11, 15]

$$ {}_0^{GL}\Delta_{k+1}^{(\nu)}\boldsymbol{x}_{k+1} = \boldsymbol{A}\boldsymbol{x}_k + \boldsymbol{B}\boldsymbol{u}_k, \tag{26a} $$

$$ \boldsymbol{y}_k = \boldsymbol{C}\boldsymbol{x}_k + \boldsymbol{D}\boldsymbol{u}_k, \tag{26b} $$

where $\boldsymbol{x}_k \in R^n$, $\boldsymbol{u}_k \in R^m$, $\boldsymbol{y}_k \in R^p$ are the state, input and output vectors, respectively. The matrices $\boldsymbol{A} \in R^{n\times n}$, $\boldsymbol{B} \in R^{n\times m}$, $\boldsymbol{C} \in R^{p\times n}\boldsymbol{D} \in R^{p\times m}$ are constant. A vector $\boldsymbol{x}_0 \in R^n$ is treated as initial condition vector. To distinguish the states of the same system evaluated by Grünwald-Letnikov and Horner forms appropriate superscripts (GL) and (H) are added. Taking into account (19b) and (19c) yields two simplified forms of (26a)

$$ {}^{GL}\boldsymbol{x}_{k+1} = -\sum_{i=1}^{k+1} a_i^{(\nu)\,GL}\boldsymbol{x}_{k+1-i} + \boldsymbol{A}^{GL}\boldsymbol{x}_k + \boldsymbol{B}\boldsymbol{u}_k, \tag{27} $$

$$ \begin{aligned} {}^{H}\boldsymbol{x}_{k+1} = \boldsymbol{A}^{H}\boldsymbol{x}_k - c_1^{(\nu)}\Big({}^{H}\boldsymbol{x}_k + c_2^{(\nu)}\Big({}^{H}\boldsymbol{x}_{k-1} + c_3^{(\nu)} \\ \cdot \Big({}^{H}\boldsymbol{x}_{k-2} + \cdots + \Big(c_{k+1}^{(\nu)}\,{}^{H}\boldsymbol{x}_0\Big)\Big)\Big)\Big) + \boldsymbol{B}\boldsymbol{u}_k. \end{aligned} \tag{28} $$

5.1. Solution of simplified forms of the FOS state-space model. In practical applications one should apply simplified forms of the FOBD described by formulae (20) or (21). This is forced by the FOBD evaluation problems caused by microcomputer finite memory sampling time. Simplified dynamical models are obtained by a substitution of coefficients (19), $c_{i,k}^{(\nu)}$ and $\widetilde{c}_{lL,k}^{(\nu)}$ into (27) and (28), respectively

$$ {}^{GL,j}\boldsymbol{x}_{k+1} = -\sum_{i=1}^{k+1} a_{j,i}^{(\nu)\,GL,j}\boldsymbol{x}_{k+1-i} + \boldsymbol{A}^{GL,j}\boldsymbol{x}_k + \boldsymbol{B}\boldsymbol{u}_k, \tag{29} $$

$$ \begin{aligned} {}^{H,j}\boldsymbol{x}_{k+1} = \boldsymbol{A}^{H,j}\boldsymbol{x}_k - c_{j,1}^{(\nu)}\Big({}^{H,j}\boldsymbol{x}_k + c_{j,2}^{(\nu)}\Big({}^{H,j}\boldsymbol{x}_{k-1} + c_{j,3}^{(\nu)} \\ \cdot \Big({}^{H,j}\boldsymbol{x}_{k-2} + \cdots + \Big(c_{j,k+1}^{(\nu)}\,{}^{H,j}\boldsymbol{x}_0\Big)\cdots\Big)\Big)\Big) + \boldsymbol{B}\boldsymbol{u}_k. \end{aligned} \tag{30} $$

Realise that due to (19b), (19c) the above forms simplify to

$$ {}^{GL,j}\boldsymbol{x}_{k+1} = -\sum_{i=1}^{lL} a_{j,i}^{(\nu)\,GL,j}\boldsymbol{x}_{k+1-i} + \boldsymbol{A}^{GL,j}\boldsymbol{x}_k + \boldsymbol{B}\boldsymbol{u}_k, \tag{31} $$

$$ \begin{aligned} {}^{H,j}\boldsymbol{x}_{k+1} = \boldsymbol{A}^{H,j}\boldsymbol{x}_k - c_{j,1}^{(\nu)}\Big({}^{H,j}\boldsymbol{x}_k + c_{j,2}^{(\nu)}\Big({}^{H,j}\boldsymbol{x}_{k-1} + c_{j,3}^{(\nu)} \\ \cdot \Big({}^{H,j}\boldsymbol{x}_{k-2} + \cdots + \Big(c_{j,lL}^{(\nu)}\,{}^{H,j}\boldsymbol{x}_0\Big)\cdots\Big)\Big)\Big) + \boldsymbol{B}\boldsymbol{u}_k \end{aligned} \tag{32} $$

appropriately.

5.2. The FOS response accuracy analysis. By definition

$$ {}_0^{GL}\Delta_k^{(\nu)} f_k = {}_0^{H}\Delta_k^{(\nu)} f_k. \tag{33} $$

In the FOS response numerical calculation by the same hardware and software, equality (33) is not always satisfied. Hence, an error function may serves as a measure of the differences between numerical values of formulae (1) and (3) obtained using the approximations (20) and (21), respectively.

$$ {}^{GL,H}e_k = \left| {}_0^{GL}\Delta_k^{(\nu)} f_k - {}_0^{H}\Delta_k^{(\nu)} f_k \right|. \tag{34} $$

This suggests that as an exact value one may consider a mean value of (1) and (3)

$$ {}_0\Delta_k^{(\nu)} f_k = \frac{{}_0^{GL}\Delta_k^{(\nu)} f_k + {}_0^{H}\Delta_k^{(\nu)} f_k}{2}. \tag{35} $$

Next one defines two error functions

$$ \begin{aligned} {}_0^{GL,j}e_k &= \left| {}_0\Delta_k^{(\nu)} f_k - {}_0^{GL,j}\Delta_k^{(\nu)} f_k \right| {}_0^{H,j}e_k \\ &= \left| {}_0\Delta_k^{(\nu)} f_k - {}_0^{H,j}\Delta_k^{(\nu)} f_k \right| \end{aligned} \tag{36} $$

which serves as a tool for optimal lL evaluation. The optimality of lL is considered as minimal values that guarantee not to exceed assumed maximal absolute error. Here one should consider two cases:

a) (asymptotically stable solution)

$$ -\infty < \lim_{k\to\infty} \boldsymbol{x}_k = \boldsymbol{x}_s < \infty, \tag{37} $$

b) (limit circle)

$$ \boldsymbol{x}_{\min} \le \lim_{k\to\infty} \boldsymbol{x}_k \le \boldsymbol{x}_{\max}. \tag{38} $$

Similarly one defines numerical errors occurring in evaluation of the simplified Horner form (32). One should note that applying simplified forms (31) and (32) one gets steady state errors (37). The solution of this model inadequacy may be extracted by a matrix $\boldsymbol{B}$ correction

5.3. Necessity of a matrix $\boldsymbol{B}$ correction. Now it is assumed that the system (26) and their approximations (31) and (32) are asymptotically stable. Moreover it is assumed that the system is subjected to an input signal preserving the steady-state of the solution [13–15]. The last statement means that the one-sided $\mathcal{Z}$-transform of the input signal $\boldsymbol{u}_k$ can be splitted into a form

$$\mathcal{Z}\{\boldsymbol{u}_k\} = \boldsymbol{U}(z) = \frac{1}{z-1}\boldsymbol{U}'(z) \tag{39}$$

with an assumption that

$$\lim_{z\to 1}\boldsymbol{U}'(z) = \boldsymbol{U}'(1) \neq \boldsymbol{0}. \tag{40}$$

To evaluate the steady-state value of the state one uses the final value theorem [14]. Hence

$$^{GL}\boldsymbol{x}_s = \lim_{k\to\infty} {}^{GL}\boldsymbol{x}_k = \lim_{z\to 1}(z-1)^{GL}\boldsymbol{X}(z), \tag{41}$$

$$^{GL,j}\boldsymbol{x}_s = \lim_{k\to\infty} {}^{GL,j}\boldsymbol{x}_k = \lim_{z\to 1}(z-1)^{GL,j}\boldsymbol{X}(z), \tag{42}$$

where ${}^{GL}\boldsymbol{X}(z)$ and ${}^{GL,j}\boldsymbol{X}(z)$ for $j = 1,2,3$ denote the one-sided Z – Transform of (26a) and (31), respectively. Applying the one-sided $\mathcal{Z}$ – Transform one obtains

$$^{GL}\boldsymbol{X}(z) = \left[z\left(1-z^{-1}\right)^{\nu}\boldsymbol{I} - \boldsymbol{A}\right]^{-1}\boldsymbol{B}\boldsymbol{U}(z), \tag{43}$$

$$^{GL,j}\boldsymbol{X}(z) = \left[z\sum_{i=0}^{lL} a_{j,i}^{(\nu)} z^{-i}\boldsymbol{I} - \boldsymbol{A}\right]^{-1}\boldsymbol{B}\boldsymbol{U}(z). \tag{44}$$

Substitution (43) and (44) into (41) yields

$$^{GL}\boldsymbol{x}_s = [-\boldsymbol{A}]^{-1}\boldsymbol{B}\boldsymbol{U}'(1). \tag{45}$$

Similar substitutions and transformations performed on formula (26a) give

$$^{GL,j}\boldsymbol{x}_s = \left[\sum_{i=0}^{lL} a_{j,i}^{(\nu)}\boldsymbol{I} - \boldsymbol{A}\right]^{-1}\boldsymbol{B}\boldsymbol{U}'(1). \tag{46}$$

To guarantee the same steady-states

$$^{GL}\boldsymbol{x}_s = {}^{GL,j}\boldsymbol{x}_s \tag{47}$$

in simplified realizations one must correct an input matrix $\boldsymbol{B}$ in (46). The corrected matrix will be denoted by $\boldsymbol{B}_j$. Then from (47) together with (45) and (46) one gets

$$[-\boldsymbol{A}]^{-1}\boldsymbol{B}\boldsymbol{U}'(1) = \left[\sum_{i=0}^{lL} a_{j,i}^{(\nu)}\boldsymbol{I} - \boldsymbol{A}\right]^{-1}\boldsymbol{B}_j\boldsymbol{U}'(1) \tag{48}$$

and after simple rearrangements

$$\boldsymbol{B}_j\boldsymbol{U}'(1) = \left[\boldsymbol{I} - \sum_{i=0}^{lL} a_{j,i}^{(\nu)}\boldsymbol{A}^{-1}\right]\boldsymbol{B}\boldsymbol{U}'(1). \tag{49}$$

In the single input systems this condition simplifies essentially to

$$\boldsymbol{B}_j = \left[\boldsymbol{I} - \sum_{i=0}^{lL} a_{j,i}^{(\nu)}\boldsymbol{A}^{-1}\right]\boldsymbol{B}. \tag{50}$$

In the light of the above investigations for the FOS approximations one proposes

$$\begin{aligned} {}^{GL,j}\boldsymbol{x}_{k+1} = &-\sum_{i=1}^{lL} a_{j,i}^{(\nu)}{}^{GL,j}\boldsymbol{x}_{k+1-i} \\ &+\boldsymbol{A}^{GL,j}\boldsymbol{x}_k + \boldsymbol{B}_j\boldsymbol{u}_k, \end{aligned} \tag{51}$$

$$\begin{aligned} {}^{H,j}\mathbf{x}_{k+1} = \mathbf{A}^{H,j}\boldsymbol{x}_k - c_{j,1}^{(\nu)}\Big({}^{H,j}\boldsymbol{x}_k + c_{j,2}^{(\nu)}\Big({}^{H,j}\boldsymbol{x}_{k-1} + c_{j,3}^{(\nu)} \\ \cdot\Big({}^{H,j}\boldsymbol{x}_{k-2} + \cdots + \Big(c_{j,lL}^{(\nu)}{}^{H,j}\boldsymbol{x}_0\Big)\cdots\Big)\Big)\Big) + \boldsymbol{B}_j\boldsymbol{u}_k. \end{aligned} \tag{52}$$

One should note that

$$\sum_{i=0}^{lL} a_{j,i}^{(\nu)} \neq 0 \quad \text{for} \quad l, L < \infty \tag{53}$$

and

$$\lim_{lL\to\infty}\sum_{i=0}^{lL} a_{j,i}^{(\nu)} = 0 \quad \text{for} \quad l, L < \infty. \tag{54}$$

The influence of the finite calculation length lL to the steady state level illustrates a following example.

5.4. Numerical example. Consider the FOS (36a) with matrices and a state vector

$$\boldsymbol{A} = \begin{bmatrix} -\frac{273}{100} & \frac{173}{40} \\ -\frac{173}{200} & \frac{73}{100} \end{bmatrix}, \qquad \boldsymbol{B} = \begin{bmatrix} 3 \\ 1 \end{bmatrix},$$

$$\nu = \frac{1}{2}, \qquad \boldsymbol{x}_k = \begin{bmatrix} x_{1,k} \\ x_{2,k} \end{bmatrix}.$$

Next one assumes that the system is subjected to the steady input signal with non-zero initial conditions

$$\boldsymbol{x}_0 = \begin{bmatrix} x_{1,0} \\ x_{2,0} \end{bmatrix} = \begin{bmatrix} 1 \\ -1 \end{bmatrix}, \qquad \boldsymbol{u}_k = \mathbf{1}_k,$$

where $\mathbf{1}_k$ denotes the discrete unit step function. In Fig. 6 the considered system state transients are plotted.

Now one analyses the simplified solution (19) with $L = 100$ and $l = 3$ and $a_{jL+i}^{(\nu)} \leq \widetilde{a}_{jL}^{(\nu)}$ for $j = 1,2,3$ and $i = 1,\ldots,L-1$. The plot of coefficients $a_{2,k}^{(\nu)}$ (in red) together with $a_k^{(\nu)}$ (in black) is presented in Fig. 7.

Below in Fig. 8 the plots of states

$$^{GL,2}\boldsymbol{x}_k = \begin{bmatrix} {}^{GL,2}x_{1,k} \\ {}^{GL,2}x_{2,k} \end{bmatrix}$$

are presented.

In Fig. 9 there are plotted errors

$$^{GL,2}e_{i,k} = {}^{GL}x_{i,k} - {}^{GL,2}x_{i,k} \quad \text{for} \quad i = 1,2. \tag{55}$$

The errors (55) limits for the approximated system with corrected matrices $\boldsymbol{B}_j$ are presented in Figs. 10a,b. The limits are visible for the time interval $[0\,30000]$. In the same figures errors obtained for approximated systems without a matrix $\boldsymbol{B}$ correction are added (in red). These errors are denoted as ${}^{GL,2,B}e_{i,k}$ for $i = 1,2$. It is clear that errors of the approximated FOS without input matrix $\boldsymbol{B}$ correction tend to non-zero steady values The correction removes this problem.

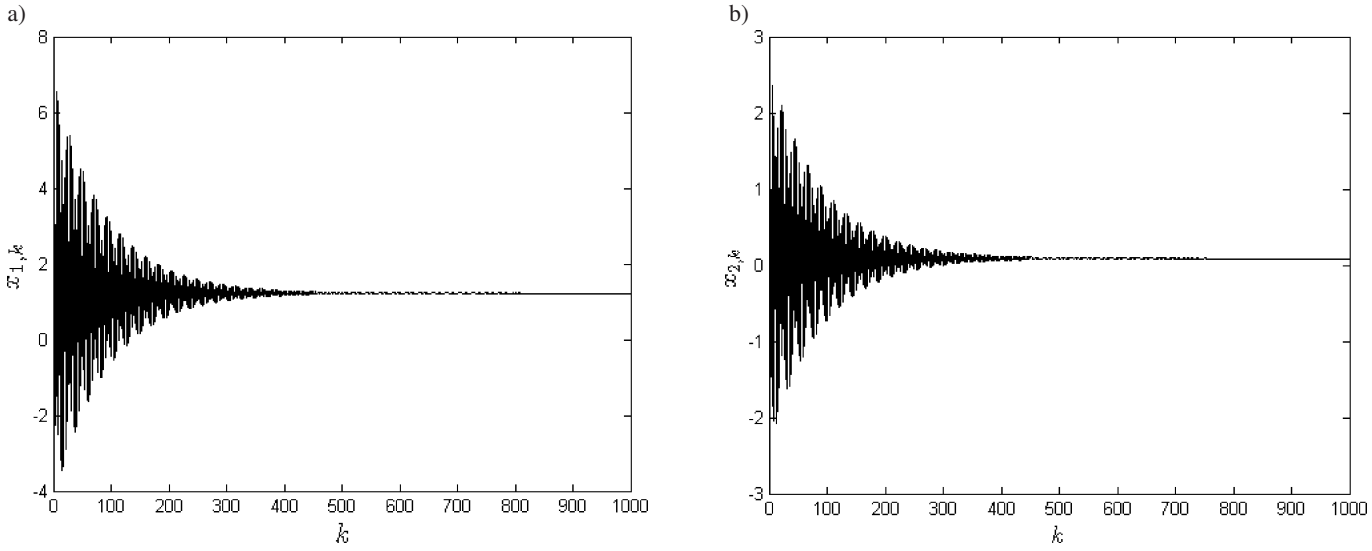

Fig. 6. The system states ${}^{GL}x_{1,k}$ ${}^{GL}x_{2,k}$ vs. discrete time

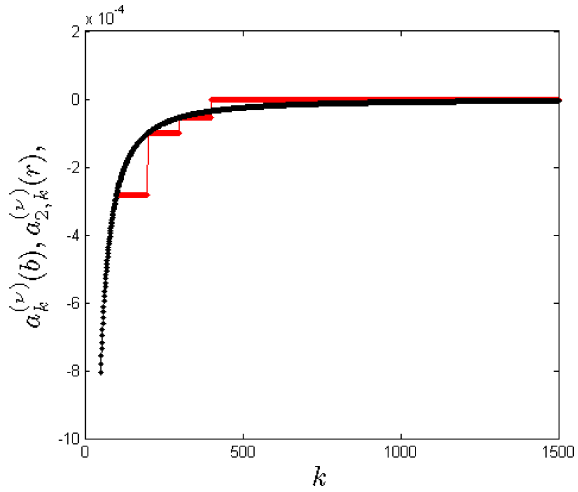

Fig. 7. Plots of coefficients $a_{2,k}^{(\nu)}$ (in red) and $a_k^{(\nu)}$ (in black)

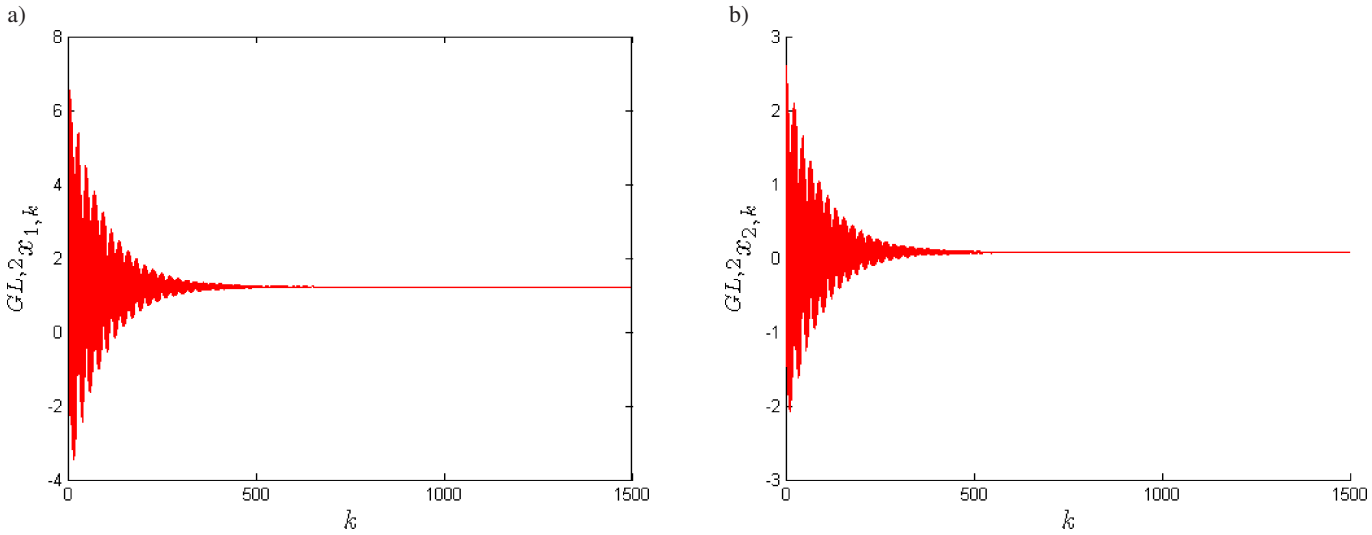

Fig. 8. Plots of states ${}^{GL,2}x_{1,k}$, ${}^{GL,2}x_{2,k}$ vs. discrete time

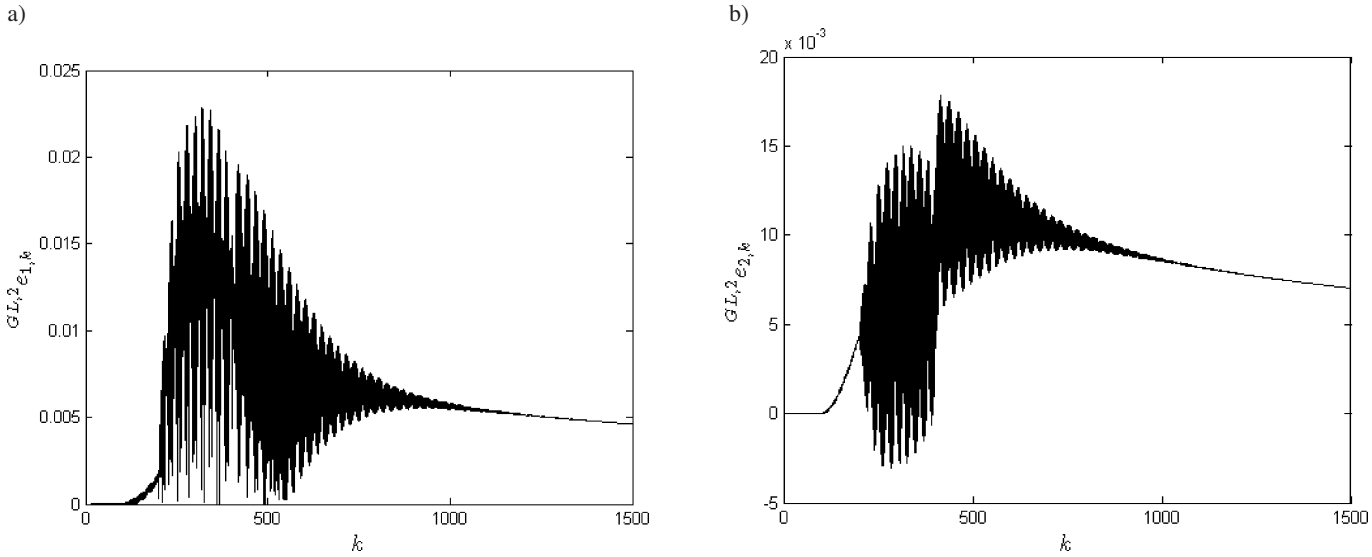

Fig. 9. Plots of errors ${}^{GL,2}e_{1,k}$, ${}^{GL,2}e_{2,k}$ vs. discrete time

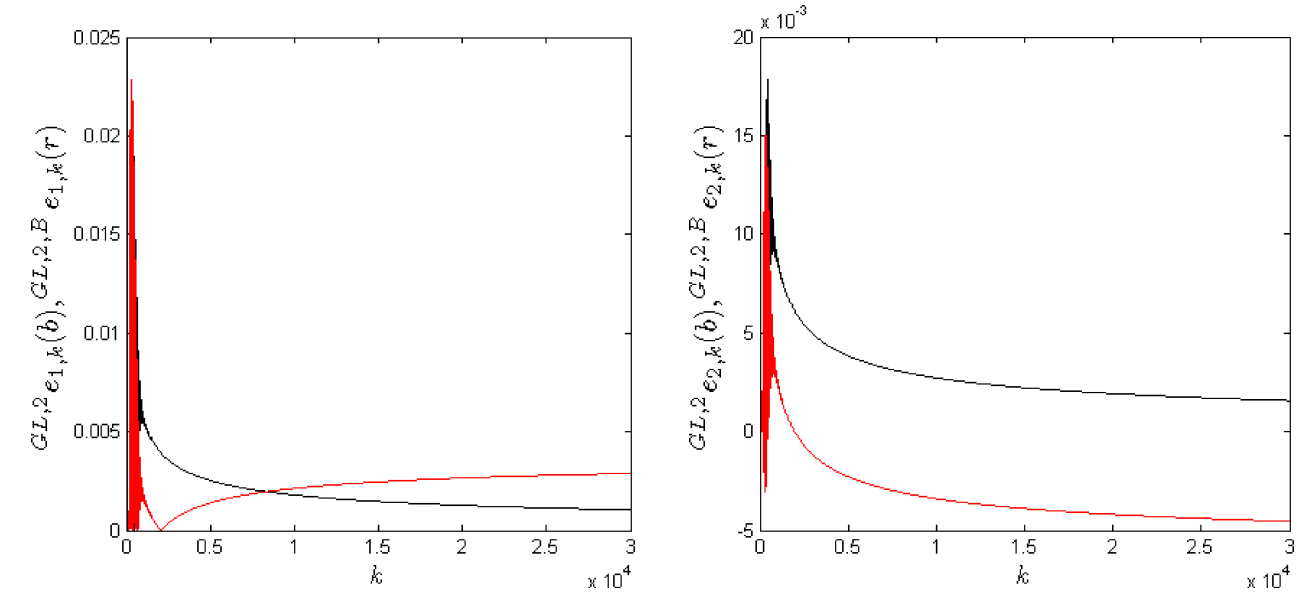

Fig. 10. Plots of errors ${}^{GL,2}e_{i,k}$, and ${}^{GL,2,B}e_{i,k}$ for $i = 1, 2$ vs. discrete time

6. Marginally stable system and its approximation

An approximation of a marginally stable FOS (or stable in the Lapunov sense) by that described by Eqs. (29) or (30) for $j = 1$ may not be an easy task. Preservation of the stability limit by an approximated system may lead to a very large L. Much greater choice give approximations defined by $j = 2, 3$. Here the key role plays an appropriate coefficients with tilde $a^{(\nu)}_{jL+i} \le \widetilde{a}^{(\nu)}_{jL} \le a^{(\nu)}_{(j+1)L}$ selection. This free choice preserves the stability limit.

6.1. Numerical example. Now one considers a system (26a) with matrices, initial conditions and input signal

$$\boldsymbol{A} = \begin{bmatrix} -\dfrac{4389}{1591} & \dfrac{1297}{295} \\ -\dfrac{1399}{1591} & \dfrac{1207}{1591} \end{bmatrix}, \qquad \boldsymbol{B} = \begin{bmatrix} 3 \\ 1 \end{bmatrix},$$
$$\nu = 0.5, \qquad \boldsymbol{x}_0 = \begin{bmatrix} 1 \\ -1 \end{bmatrix}, \qquad u_k = 0. \tag{56}$$

One may check that the system is marginally stable [9–12]. The limit cycle is presented in Fig. 11.

In Figs. 12 and 13 the plots of solutions (27) and (51) for $j = 2$, $L = 171$ and $l = 3$ are presented, respectively. To preserve the approximated system stability limit as the last nonzero coefficient in (19b) there were taken $\widetilde{a}^{(0.5)}_{lL} = 0.78363 a^{(0.5)}_{lL}$.

In Fig. 14 errors (55) are given.

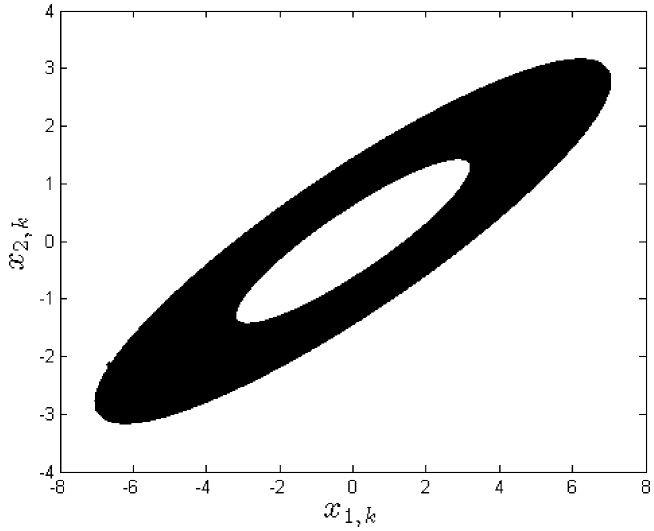

Fig. 11. The system (56) limit circle simulated over time interval $[0\,120000]$

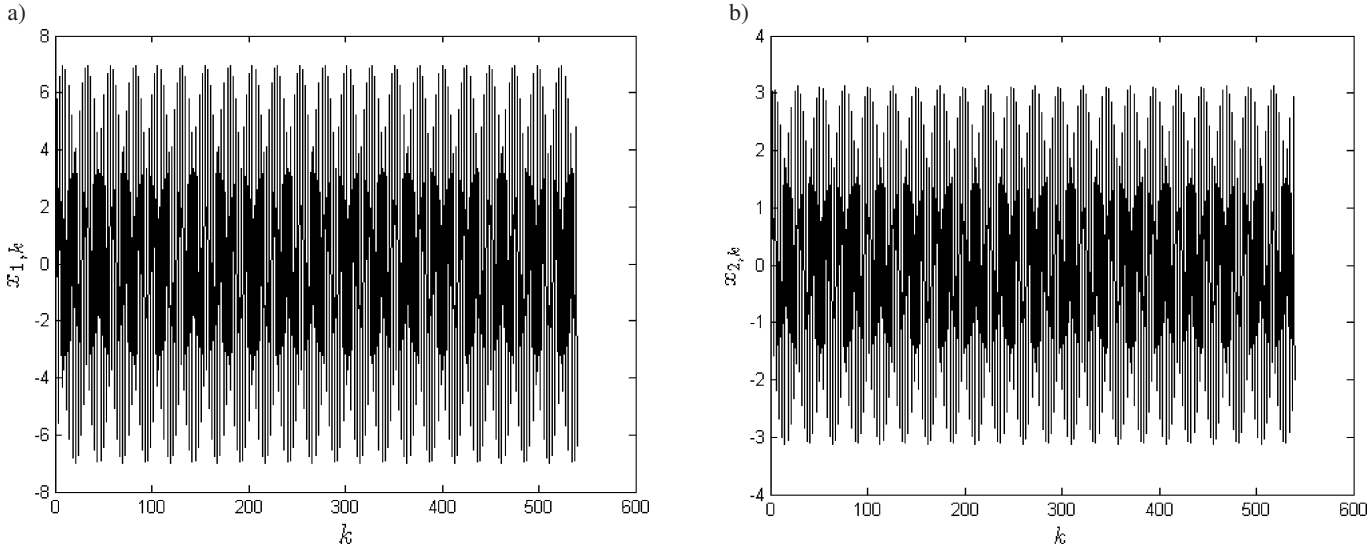

Fig. 12. The system states ${}^{GL}x_{1,k}$ ${}^{GL}x_{2,k}$ vs. discrete time

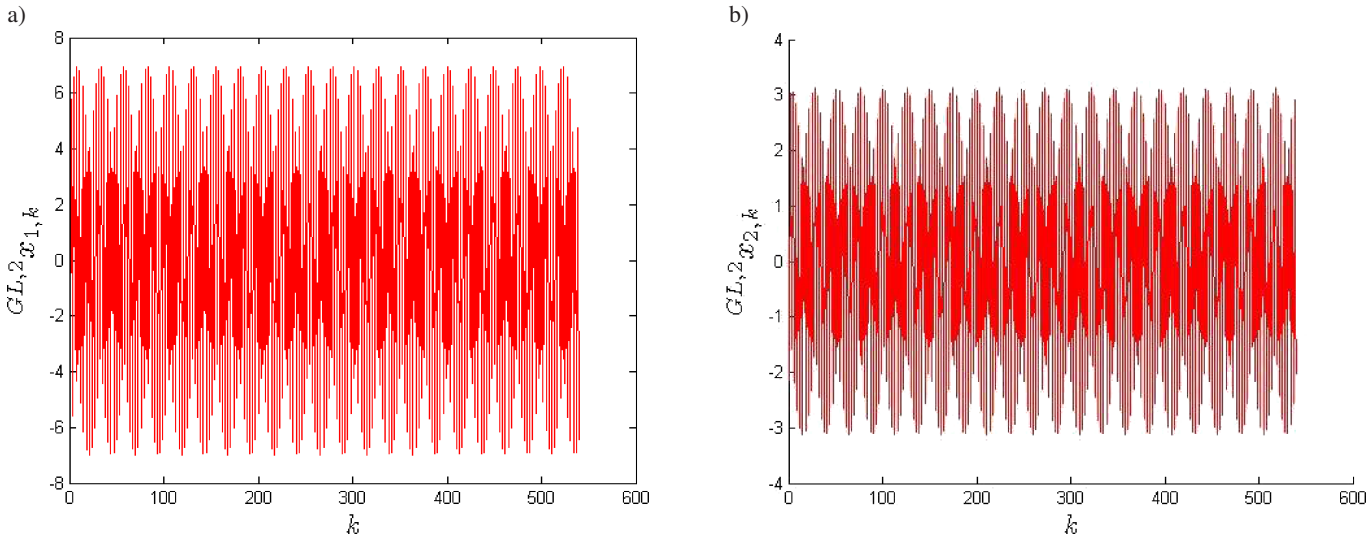

Fig. 13. Plots of states ${}^{GL,2}x_{1,k}$, ${}^{GL,2}x_{2,k}$ vs. discrete time

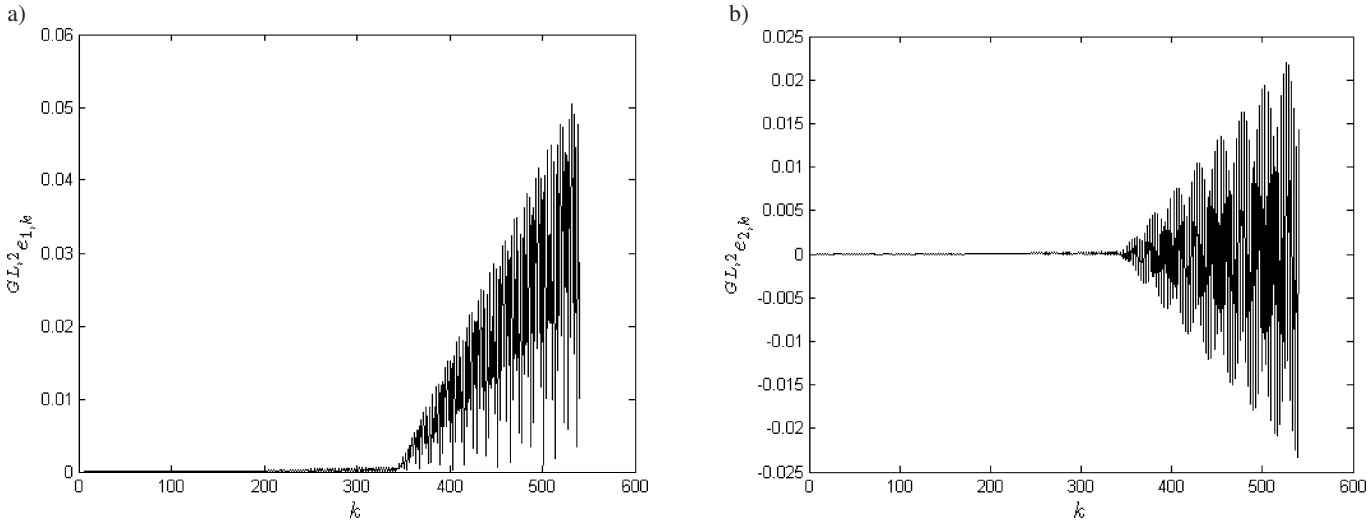

Fig. 14. Plots of errors $^{GL,2}e_{1,k}$, $^{GL,2}e_{2,k}$ vs. discrete-time

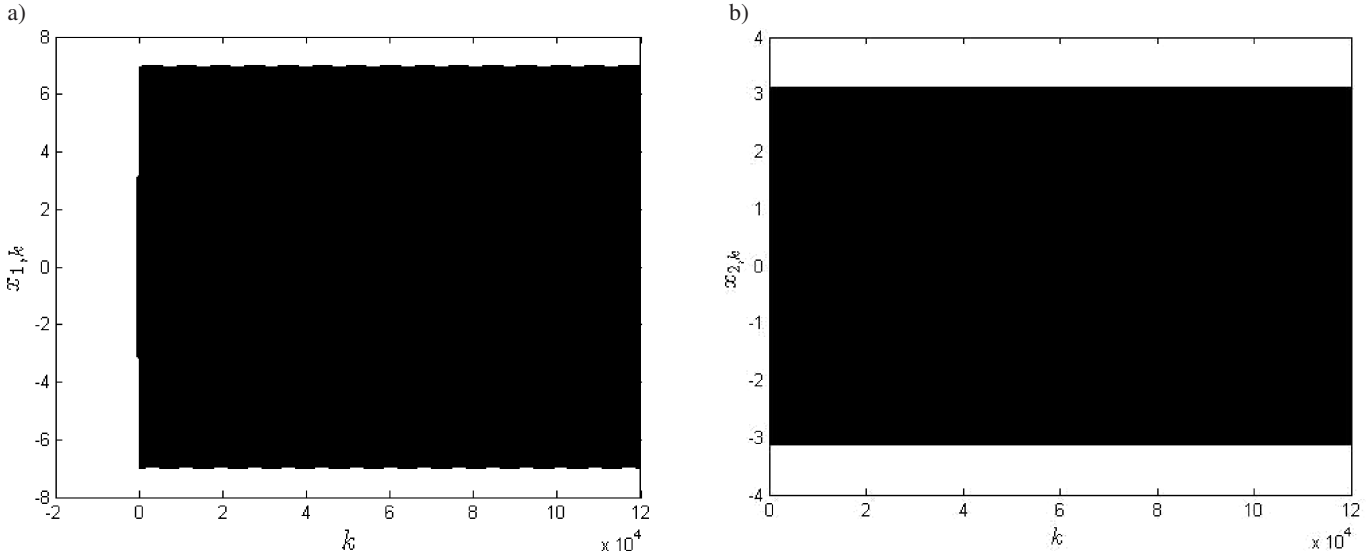

Fig. 15. The system states $^{GL}x_{1,k}$ $^{GL}x_{2,k}$ over the time interval [0 120000]

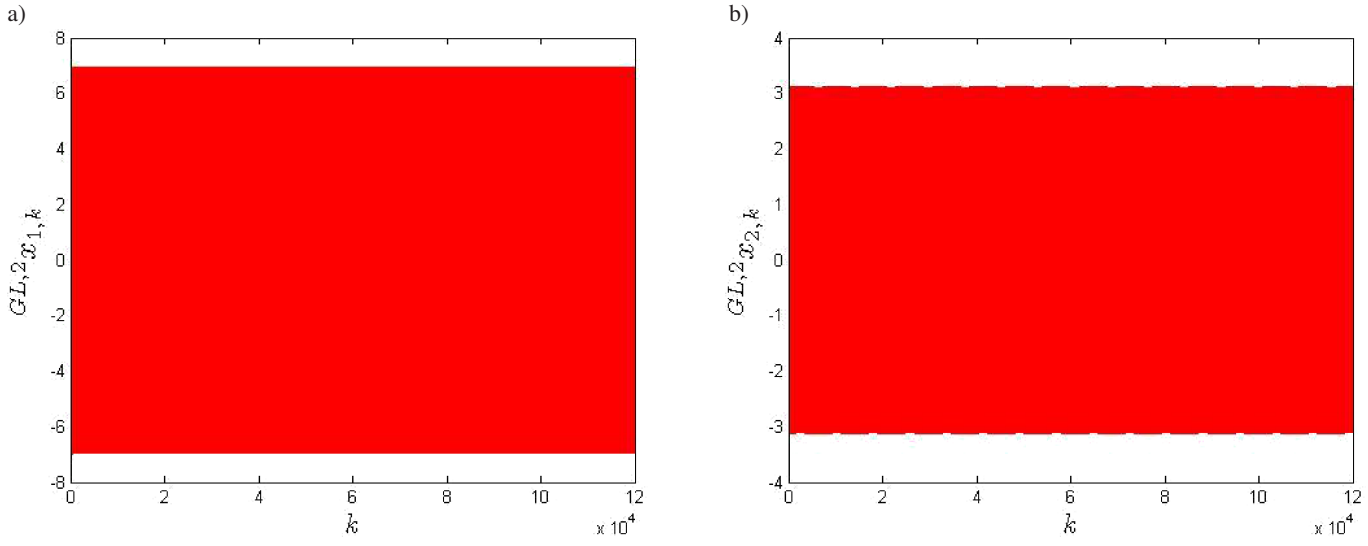

Fig. 16. Plots of states $^{GL,2}x_{1,k}$, $^{GL,2}x_{2,k}$ over the time interval [0 120000]

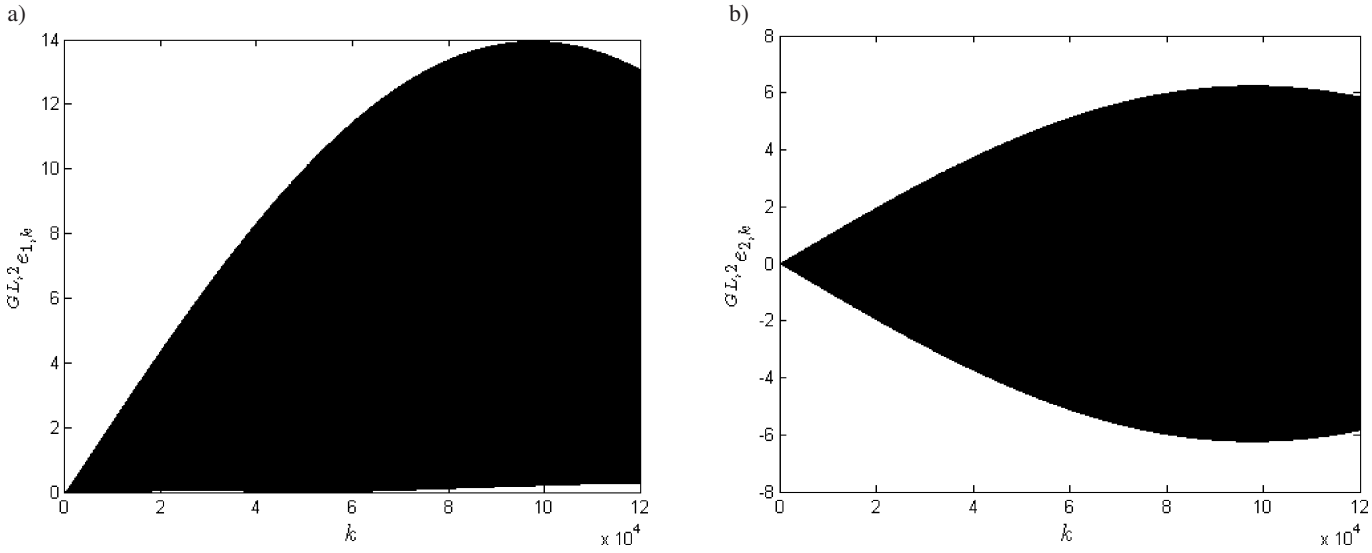

Fig. 17. Plots of errors $^{GL,2}e_{1,k}$, $^{GL,2}e_{2,k}$ over the time interval $[0\,120000]$

In marginally stable systems it is important a transient behaviour over a large time interval. Figures 15–17 present the same plots as in Figs. 12–14 but over the larger range $[0\,120000]$.

7. Concluding remarks

The problem of the FOBD approximations by the integer high-order models has been investigated in this paper. The approximation problem arises in the practical microprocessor evaluation of the FOBD for instance in the FO PID controller. The proposed simplified forms parameters L and l may be selected according to frequency criteria. Investigations pointed out the necessity of an approximated model constant gain correction. Second numerical example shows the difficulty in approximation of the FOS which is marginally stabile. Though one may achieve the same amplitudes of oscillating steady state response the phase shift is inevitable.

REFERENCES

[1] T. Kaczorek, *Selected Problems of Fractional Systems Theory*, Springer, London, 2010.

[2] K. Miller and B. Ross, A*n Introduction to Fractional Calculus and Fractional Differential Equations*, Wiley, New York, 1993.

[3] K.B. Oldham and J. Spanier, *The Fractional Calculus*, Academic Press, New York, 1974.

[4] A. Oustaloup, O. Cois, and L. Lelay, *Représentation et Identification par Modèle non Entire*, Hermes, Paris, 2005.

[5] I. Podlubny, *Fractional Differential Equations*, Academic Press, New York, 1999.

[6] A. Kilbas, H. Srivastava, and J. Trujillo, *Theory and Applications of Fractional Differential Equations*, Elsevier, Amsterdam, 2006.

[7] P. Ostalczyk, "The non-integer difference of the discrete-time function and its application to the control system synthesis", *Int. J. System Science* 31, 1551–1561 (2000).

[8] P. Ostalczyk, "Fractional-order backward difference equivalent forms", in *Fractional Differentiation and Its Applications, Systems Analysis, Implementation and Simulation, System Identification and Control*, pp. 545–556, Ubooks Verlag, Neusäß, 2005.

[9] S.M. Kuo, B.H. Lee, and W. Tian, *Real-time Digital Signal Processing: Fundamentals, Implementations and Applications*, Wiley, Chichester, 2013.

[10] M. Busłowicz and A. Ruszewski, "Necessary and sufficient conditions for stability of fractional discrete-time linear state-space systems", *Bull. Pol. Ac.: Tech.* 61 (4), 779–786 (2013).

[11] A. Dzieliński and D. Sierociuk, "Stability of discrete fractional order state-space systems", *J. Vibration and Control* 14, 1543–1556 (2008).

[12] M. Busłowicz and T. Kaczorek, "Simple conditions for practical stability of linear positive fractional discrete-time linear systems", *Int. J.Applied Mathematics and Computer Sciences* 19 (2), 263–269 (2009).

[13] R. Stanisławski and K.J. Latawiec, "Stability analysis for discrete-time fractional-order LTI state-space systems. Part I: new necessary and sufficient conditions for asymptotic stability", *Bull. Pol. Ac.: Tech.* 61 (2), 353–361, (2013).

[14] K. Ogata, *Discrete-Time Control Systems*, Prentice-Hall Int.Editions, Englewood Cliffs, 1987.

[15] D. Valério and J. da Costa, *An Introduction to Fractional Control*, The Institution of Engineering and Technology, London, 2013.